Chem-Bio Informatics Journal, Vol. 3, No. 2, pp.46-57(2003)

Conformational Analysis and Docking Study of Potent Acetylcholinesterase Inhibitors Having a Benzylamine Moiety

Narihiro Toda[1], Yoriko Iwata[1], Keiko Tago[1], Hiroshi Kogen[1], Tsugio Kaneko[2] and Shuichi Miyamoto[1*]

[1]Exploratory Chemistry Research Laboratories and [2]Neuroscience and Immunology Research Laboratories, Sankyo Co., Ltd., 1–2–58, Hiromachi, Shinagawa-ku, Tokyo 140-8710, Japan

**E-mail: miyamoto11@hq.sankyo.co.jp*

(Received March 11, 2003; accepted May 14, 2003; published online May 31, 2003)

Abstract

A conformational analysis and docking study of nitrophenoxyalkylbenzylamine derivatives with inhibitory activities against acethylcholinesterase was carried out in an attempt to analyze their structure–activity relationships based on the enzyme–inhibitor interaction. First, stable conformers of the inhibitors alone were obtained from the conformational analysis by molecular dynamics. Next, a docking study of the inhibitors into the ligand binding site was performed. Among the resulting stable complex structures, it was found that in the case of the two stereoisomers with a 7-membered ring, the more active one of the two formed a much more stable complex structure. On the other hand, complex structures with comparable energies were obtained for both stereoisomers that had no 7-membered ring and showed similar inhibitory activities. Lastly, structural features of the complex models of a series of inhibitors with side chains of different lengths were evaluated and corresponded well to their inhibitory activities.

Key Words: conformational analysis, docking study, molecular mechanics, molecular dynamics, acethylcholinesterase inhibitor, structure–activity relationship, nitrophenoxyalkylbenzylamine, stereoisomer

Area of Interest: Molecular Recognition

1. Introduction

Alzheimer's disease (AD), the most common cause of dementia, is a neurodegenerative disorder characterized by a progressive deterioration of memory and cognition [1][2]. Enhancement of the central cholinergic function by the inhibition of acetylcholinesterase (AChE) is, so far, the only clinically effective approach for the treatment of AD [3][4]. However, the clinical usefulness of marketed AChE inhibitors (AChEIs) is limited, mainly due to the adverse effect on peripheral organs [5][6]. AD patients often exhibit psychiatric symptoms such as irritability, anxiety, and

depression. Depression in AD patients has been successfully treated with inhibitors of the serotonin transporter (SERT) [7], anti-depressants that have no anti-cholinergic action. Thus, it is anticipated that drugs exhibiting SERT and AChE inhibitory activities could offer greater therapeutic benefits because the anti-depressive effect due to SERT inhibition might reduce the demand on cholinergic systems in the brain and ameliorate cognitive deficits. These dual inhibitors would be a novel class of anti-AD drugs and be more effective in alleviating the symptoms of AD than other known AChE inhibitors.

In the search for such dual inhibitors, we have synthesized benzylamine derivatives that have a highly efficient dual inhibition profile (Figure 1). Interestingly, compound **1** with a 7-membered ring exhibited stereoselectivity against AChE (IC_{50} = 609 (*S*) vs 14 (*R*) nM). On the other hand, little difference in AChE inhibitory activities was observed for the stereoisomers of compound **2**, which has no 7-membered ring, i.e., has an open substructure. With regard to compounds **2**–**4**, which have different lengths of the alkyl chain between the benzylamine and nitrophenoxy moieties (Y), compound **3** with the shortest tether group showed weak inhibitory activity (IC_{50} = >1000 nM) while reasonable inhibitory activities were observed for the other compounds **2** (IC_{50} = ~100 nM) and **4** (IC_{50} = 77 nM).

With respect to donepezil, marketed as Aricept for the treatment of AD, complex structure models and energetics of its stereoisomers with comparable inhibitory activities against AChE were presented [8][9][10]. The complex crystal structure of donepezil was recently solved [11] and it was revealed that the overall binding mode predicted by the above modeling was correct although some binding interactions could not be perfectly estimated. Thus, docking study has been one of the effective tools to elucidate a ligand–enzyme binding orientation.

Since the determination of the crystal structure of AChE from *Torpedo californica* by Sussman *et al*. [12], complex structures with different ligands have been elucidated and registered in the Protein Data Bank [13]. The AChE enzyme is an α/β protein that contains 537 amino acids. The catalytic triad comprising residues Ser200, His440 and Glu327 is located at the bottom of a deep

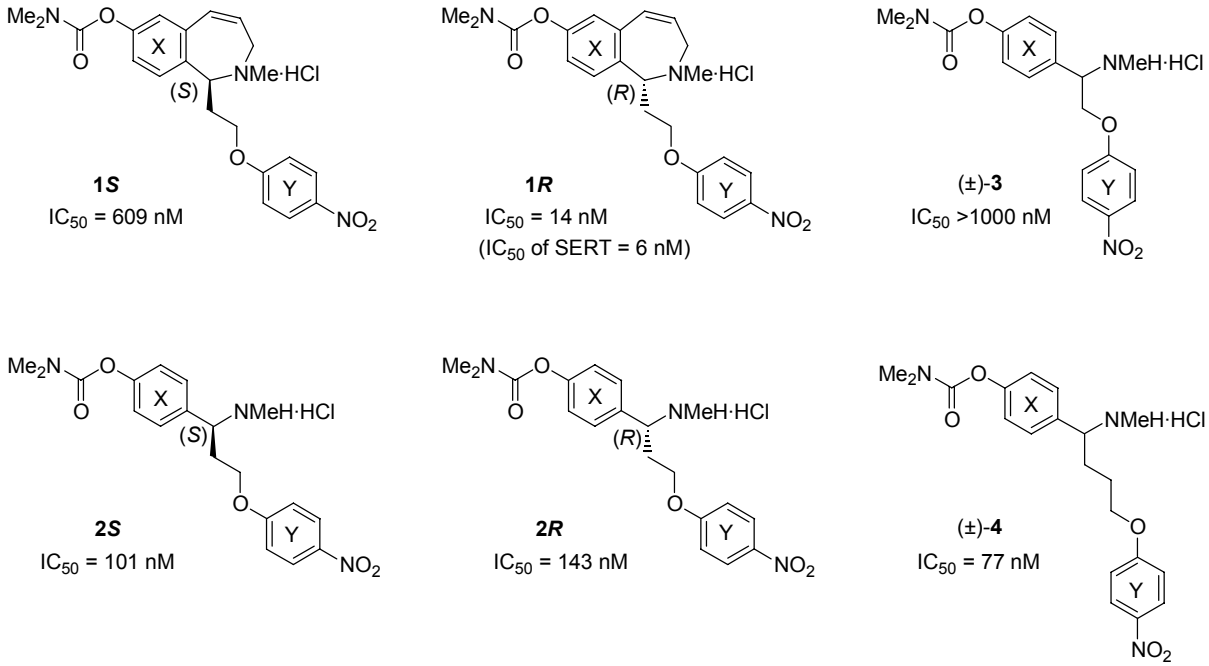

Figure 1. Chemical structures of benzylamine derivatives and their inhibitory activities against AChE.

and narrow pocket, about 20 Å long. This pocket or gorge extends halfway into the enzyme and widens out at the base. The middle of the cavity is as narrow as 4.5 Å due to the side chain of Tyr121 and the gorge is lined with the side chain rings of 14 aromatic residues. Most ligands (inhibitors) as observed from their crystal structures, are located at the bottom of the pocket, which is wide (hydrophobic pocket base), although larger ligands such as decamethonium [14] and donepezil [13] extend to the mouth of the gorge (hydrophobic pocket opening).

Recently, Bar-on *et al*. [15] reported the structual studies on the interaction of AChE and rivastigmine which possessed a carbamate moiety in the same manner as inhibitors **1**−**4**. From the aspect of structual similarity, inhibitors **1**−**4** are considered to be pseudo-irreversible inhibitors of AChE. However, preliminary experimental results [16] suggested that inhibition type of compound **2** was more like a reversible AChE inhibitor, such as donepezil, than a pseudo-irreversible inhibitor, such as rivastigmine. Therefore, we performed this study by taking inhibitors **1**−**4** as reversible AChE inhibitors.

In this article, we report the results of the conformational analysis and the docking study of inhibitors **1**−**4** with AChE in order to analyze their AChE inhibition potencies, which include difference in AChE inhibitory activity of the stereoisomers of **1**, based on their predicted enzyme−inhibitor interaction. The synthesis and full details of the biological evaluation of the inhibitors are presented elsewhere [17]. First, the conformational analysis of the inhibitors was carried out by molecular dynamics simulations to obtain their stable conformers. Next, a docking study of the inhibitors into the gorge of AChE was performed. Based on the complex structure models of the stereoisomers of compounds **1** and **2**, the interaction energies between AChE and the inhibitors were estimated and compared with their inhibitory activities. Furthermore, the structural features of the complex models of compounds **2**−**4**, which all have side chains of different lengths, were analyzed and compared with their inhibition potencies. This study would bring useful information for further development of potent AChE inhibitors.

2. Methods

2.1 Conformational analysis of inhibitors

Each molecule was model-built using the QUANTA system [18] in the protonated form with respect to the basic amine. Since compound **1** contains a tertiary methylamine moiety as a part of the 7-membered ring, the stereochemistry was taken into account by equating the nitrogen atom to a chiral carbon atom, i.e., the two stereoisomers, *R'* and *S'* were considered. Four models of **1*RR'***, **1*RS'***, **1*SR'*** and **1*SS'*** were therefore built for **1** and two models of *R* and *S* isomers were considered for the others (Figure 2). Atomic partial charges were assigned using the "Template Charge" in QUANTA. A distance-dependent dielectric constant of 4r was used in the calculation of electrostatic energy.

A conformational analysis using molecular dynamics and molecular mechanics was performed using the CHARMm force field [19]. The model was heated to 1000 K for 2 ps followed by an equilibration of 10 ps. A production run of 1000 ps was then carried out. A time step of 1 fs was used and the coordinates were saved every 0.2 ps. The saved structures were geometry-optimized by molecular mechanics with the Adopted-Basis Newton Raphson algorithm [20]. The above procedure was taken from our previous study, in which reasonable conformational search results of drug-like molecules were obtained [21]. A cluster analysis of the resulting stable conformers was done using the Group program [22] based on the torsional angles with a threshold of 30° as shown in Figure 2. The above calculations were carried out for **1*RR'***, **1*RS'***, **2*R***, **3*R*** and **4*S*** and the

resulting unique conformers were converted into their mirror images to give **1*SS'***, **1*SR'***, **2*S***, **3*S*** and **4*R***, respectively.

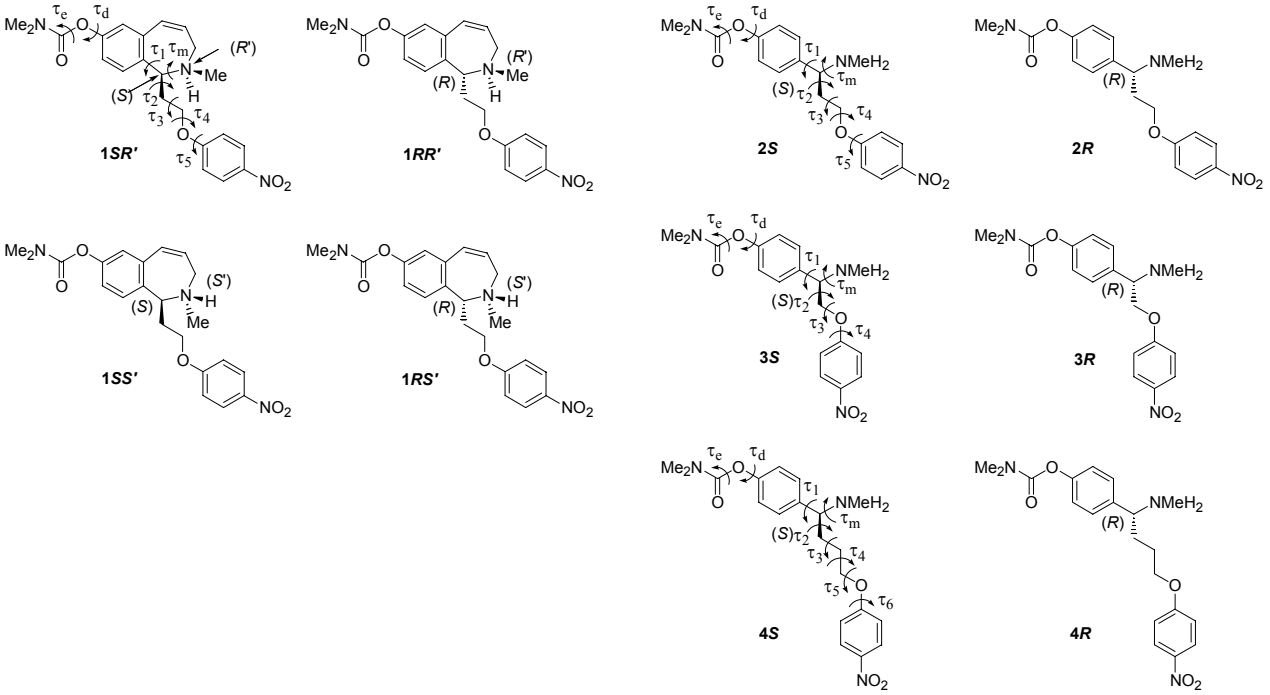

Figure 2. Model structures and torsional angle definitions of compounds used in this study.

2.2 Enzyme structure

Several X-ray crystal structures of AChE have been elucidated and were quite similar. The crystal structure of the complex with donepezil which is similar in molecular size to our compounds, was used in this study. Its code name in the PDB is 1eve and its crystallographic resolution is 2.5 Å [13]. The structure of AChE from the electric ray *Torpedo californica* (1eve) has high homology with that of mouse AChE (used for the inhibition assays in this study) and the residues constituting the binding site are highly conserved. The His, Asn and Gln side chains were analyzed using the Guess_NOHQ program [23]. Some terminal conformations were flipped when they were built the wrong way and suitable protonation forms of the imidazole ring were determined.

2.3 Docking study of the inhibitors into the ligand binding site of AChE

The docking study of the inhibitors was carried out with the QUANTA/CHARMm system based on several low energy conformations obtained by the conformational analysis. A series of initial positions and conformations of the inhibitors were manually set and stable complex structures were obtained by energy minimization with the enzyme structure being fixed. Adopted-Basis Newton Raphson algorithm was used for the energy-minimization and a distance-dependent dielectric constant of 4r was adopted. The interaction energy was estimated by simply subtracting the conformational energies of the enzyme and the isolated ligand from that of the complex. The global minimum energy obtained by the conformational analysis was employed as the conformational energy of the isolated inhibitor. In the actual derivation of the interaction

energy, the conformational energy of the enzyme was not subtracted because it was common to all complex structures.

3. Results and Discussion

3.1 Conformational analysis of inhibitors

A conformational analysis with molecular dynamics was performed for **1*RR'***, **1*RS'***, **2*R***, **3*R*** and **4*S***. The number of the resulting unique conformers with ΔE<10 kcal/mol were 170, 161, 274, 105 and 610, respectively, which is reasonable considering the flexibility of the compounds. Four kinds of conformations of the 7-membered ring of **1*RR'*** and **1*RS'*** were observed as shown in Figures 3 and 4, respectively. Two of them had a chair-like (chair) puckering and the other two had a boat-like (boat) puckering. Alternatively, half of them had the methyl substituent in the equatorial

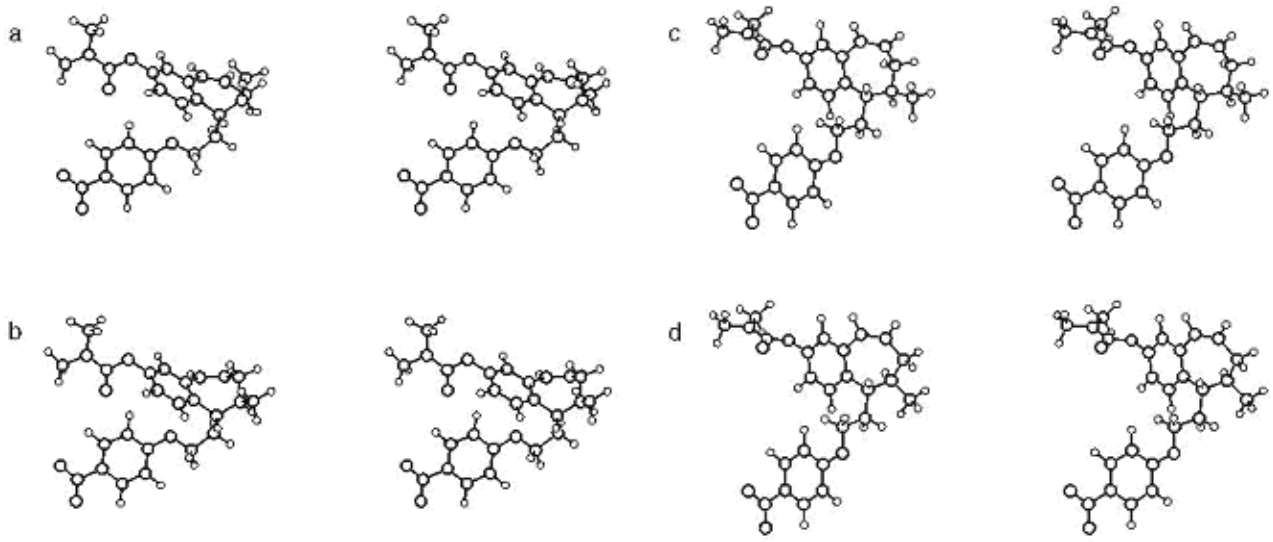

Figure 3. Stereofigures of four kinds of stable conformations of **1*RR'***.

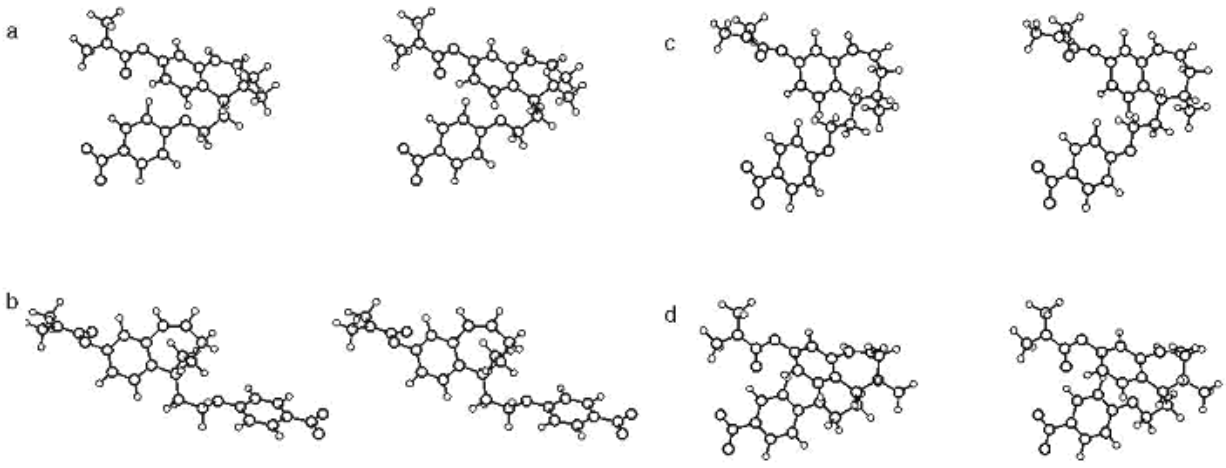

Figure 4. Stereofigures of four kinds of stable conformations of **1*RS'***.

position and the other half, in the axial position. As it can be seen from those figures, the most stable conformation had the chair-like puckering with an equatorial methyl group. Figure 5 shows representative conformations including the global minimum conformation of each of **2*R***, **3*R*** and **4*S***. The stable conformations of **1*SS'***, **1*SR'***, **2*S***, **3*S*** and **4*R*** were obtained as mirror images of those of **1*RR'***, **1*RS'***, **2*R***, **3*R*** and **4*S***, respectively.

As it can be seen from Figures 3, 4 and 5, most molecules had a compactly folded hairpin conformation with the two benzene rings in close proximity, in the global minimum structures. However, extended conformations with the two benzene rings apart (ΔE = ~2 kcal/mol) were also observed. Judging from the size of the gorge, extended conformations was used in next docking study to AChE as described below.

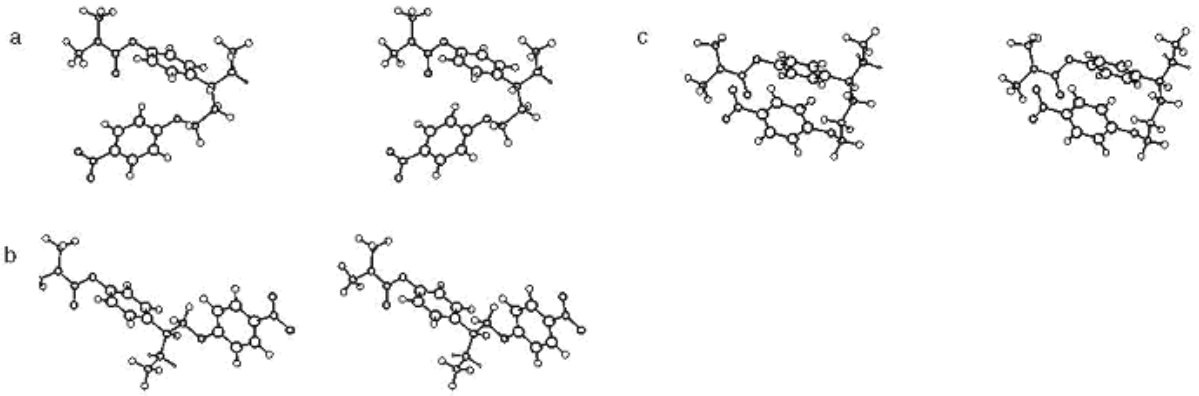

Figure 5. Stereofigures of the stable conformations of **2*R*** (a), **3*R*** (b) and **4*S*** (c).

3.2 Docking models with inhibitors bound to AChE

The size of the gorge base where the catalytic triad resides is too small for the inhibitors to fit in their folded conformations. On the other hand, inhibitors in their extended conformations with the two benzene rings apart were found to fit into the long gorge, with the dimethylcarbamate (dMC) phenyl head group (X) at the base and the nitrophenyl tail group (Y) at the opening (forward), or *vice versa* (reverse). Such an extended conformation of the ligand has been seen in the crystal structures of decamethonium and donepezil. Although the two types of orientations were initially considered, the forward orientation was found to be more favorable than the reverse orientation with respect to energetics and, therefore, only the forward orientation was employed afterwards. Considering the shape complementarity between the gorge base and the ligand head group (X) corresponding to the benzyl group of donepezil, four possible inhibitor binding modes (A, B, C and D) were examined as shown schematically in Figure 6. In these binding modes, phenyl head group (X) is aligned along one of the two larger sides of the base having a triangular transection, in the similar fashion observed in the complex of donepezil. In addition, two opposite conformations of dMC (upper and lower) were investigated. The conformation of the tether between the two phenyl rings was also examined. However, the conformational allowance was rather limited due to the narrow nature of the middle of the gorge. With regard to **1**, four kinds of conformations of the 7-membered ring were taken into account. After the manual positioning of the inhibitors, complex structures were energy-minimized with the enzyme structure being fixed. The interaction energies and conformational energies of the representative complex structures including the most stable forms of each model are compiled in Table 1.

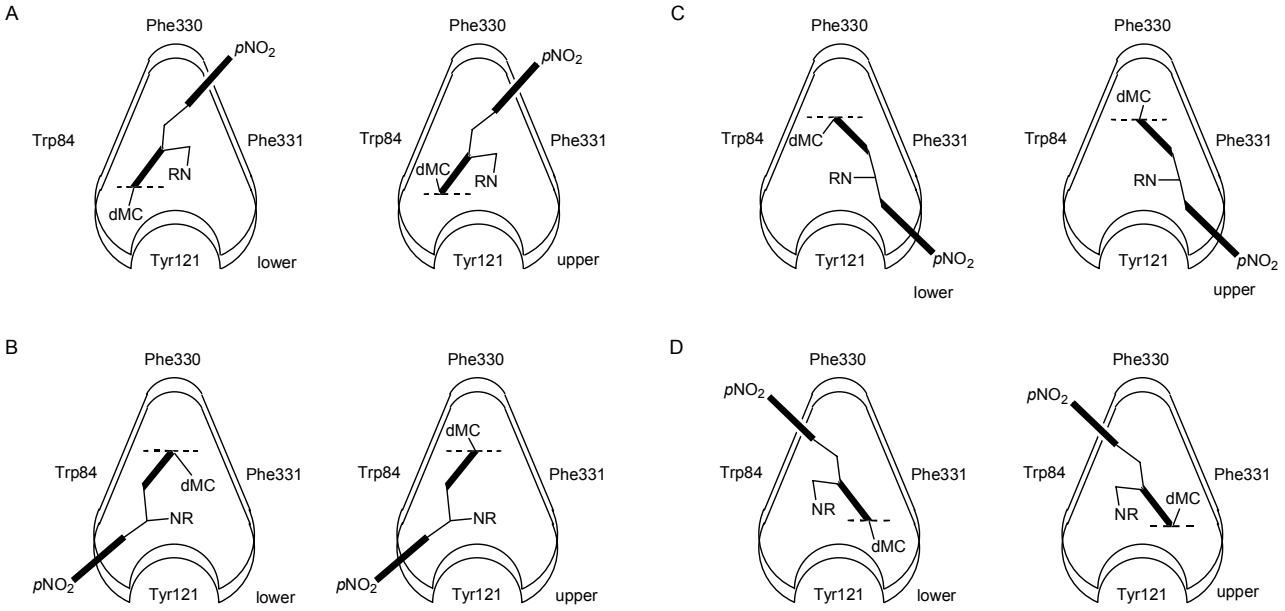

Figure 6. Schematic representation of four possible binding modes (A, B, C and D) and two conformations (upper and lower) of dMC group at the base with respect to the cross sectional plane. Transection of the enzyme gorge viewed from the opening toward the base.

3.3 Comparison between docking models of isomers of 1 and 2 and their inhibitory potencies

The interaction energies in Table 1 are regarded as approximations of the binding enthalpies without consideration of the solvation effect. The affinity or the free binding energy of a ligand is calculated by the summation of the binding enthalpy as well as the solvation effect and the change in entropy upon binding. The difference in the free binding energies between **2*S*** and **2*R*** can be approximately evaluated to be the interaction energies (E_{int}) presented in Table 1 since the contributions of the solvation effect and entropy are essentially the same for both enantiomers. In comparison with the diastereomers **1*RS'***, **1*RR'***, **1*SS'*** and **1*SR'***, the entropy contribution is also essentially the same while the contribution of the solvation effect is considered to be comparable since the area and nature of molecular surface are approximately the same. Therefore, the interaction energies (E_{int}) of the diastereomers of **1** can be estimated as the difference in the free binding energies.

As it can be seen from Table 1, with respect to compound **1** isomers, their rank order in terms of interaction energy was **1*RS'*** (most favorable) < **1*RR'*** < **1*SS'*** < **1*SR'***. Due to the freely invertible nitrogen atom, **1*R*** can favorably form the complex as **1*RS'***, and **1*S*** as **1*SS'***. The most stable model of **1*R*** with the lowest energy was about 6 kcal/mol more stable than that of **1*S***, which is consistent with the observed potencies of the isomers of **1**, i.e., **1*R*** is around 40 times more potent than **1*S***. On the other hand, comparable interaction energies were derived for **2*R*** and **2*S***. This is consistent with the fact that only a slight difference was observed for the IC_{50} values of the isomers of **2**. Overall, the docking study energetics corresponded well to the observed IC_{50} values of the isomers of both **1** and **2**. It is speculated that the rigidity of the 7-membered ring of **1*S*** may cause steric hindrance while that of flexible compound **2** may not. This structure–activity relationship is further discussed in the following structural analysis.

Table 1. Summary of energy calculations for complex models of AChE and inhibitors **1**−**4**

[a]Binding modes as defined in Figure 6. [b]Dimethylcarbamate group. [c]Puckering of the 7-membered ring. [d]Conformation of the methyl group on N atom. [e]Interaction energy

Compound	Binding mode[a]	dMC[b] (τ_d)	Puckering[c]	NMe[d] (τ_m)	τ_1	τ_2	τ_3	τ_4	Energy (kcal/mol)		
									$E_{complex}$	E_{ligand}	E_{int}[e]
1*RS'*	C	lower	boat	eq	tr	tr	tr	tr	-21.7	28.3	-50.0
	C	lower	chair	ax	tr	tr	tr	tr	-20.9		-49.2
	A	lower	chair	ax	tr	tr	tr	tr	-17.1		-45.4
1*RR'*	C	lower	boat	ax	tr	tr	g+	tr	-20.9	28.1	-49.0
	C	lower	chair	ax	tr	tr	g+	tr	-20.5		-48.6
	D	lower	chair	ax	tr	tr	tr	g+	-18.6		-46.7
1*SS'*	C	lower	boat	ax	tr	tr	g-	tr	-16.2	28.1	-44.3
	A	lower	chair	ax	tr	tr	tr	tr	-15.5		-43.6
	C	lower	chair	ax	tr	tr	g-	tr	-14.8		-42.9
1*SR'*	A	lower	boat	ax	tr	tr	g+	tr	-15.1	28.3	-43.4
	B	lower	boat	ax	tr	tr	g-	tr	-14.9		-43.2
	D	lower	boat	ax	tr	tr	g-	tr	-14.8		-43.1
2*S*	A	lower	-	g-	g+	tr	tr	tr	-38.8	9.4	-48.2
	D	lower	-	g-	g+	tr	g-	tr	-36.9		-46.3
	C	upper	-	g-	g+	tr	g-	tr	-36.2		-45.6
2*R*	D	lower	-	g-	tr	tr	tr	g+	-38.4	9.4	-47.8
	C	lower	-	g-	tr	tr	tr	tr	-38.0		-47.4
	D	upper	-	g-	tr	tr	tr	g+	-35.6		-45.0
3*S*	A	lower	-	g+	tr	tr	tr	-	-42.8	9.1	-51.9
	C	lower	-	g+	tr	tr	tr	-	-40.7		-49.8
	D	upper	-	g-	g+	tr	tr	-	-40.6		-49.7
3*R*	B	lower	-	g-	tr	tr	tr	-	-39.4	9.1	-48.5
	B	upper	-	g-	tr	tr	tr	-	-38.9		-48.0
	D	lower	-	g-	tr	tr	tr	-	-37.9		-47.0
4*R*	C	lower	-	g-	tr	tr	g+	tr	-38.3	7.4	-45.7
	D	lower	-	g-	g+	tr	g-	tr	-38.2		-45.6
	C	lower	-	tr	tr	tr	tr	tr	-37.8		-45.2
4*S*	D	lower	-	tr	tr	tr	tr	g+	-39.7	7.4	-47.1
	C	lower	-	g+	tr	tr	tr	tr	-38.7		-46.1
	B	lower	-	g-	g-	tr	tr	tr	-37.7		-45.1

Figure 7 illustrates the most stable complex structure models of **1*R*** (1st entry of **1*RS'*** in Table 1) and **2*S*** (1st entry of **2*S*** in Table 1). As it can be seen from Figure 7A, the benzoazepine ring of

1*R* was located in the hydrophobic pocket near Trp84 and Phe330. The proton of the tertiary ammonium group of the azepine ring did not directly interact with the carboxyl group of Asp72. The positive charge should have been stabilized by the negative charge of Asp72 (the NH---O distance is 5.0 Å) and the aromatic ring of Tyr334 through the aromatic–ammonium interaction [24][25]. This kind of interaction is observed by several complex crystal structures such as those of donepezil [13] and galanthamine [26]. The carbamate moiety was located near Tyr 130 and catalytic Ser200. Two torsional angles τ_3 and τ_4 in the ethoxy spacer adopted a *trans* conformation. The nitrophenyl tail group (Y) was near the indole ring of Trp279, which is located in the hydrophobic pocket opening, and the nitro group was rather exposed to the solvent. The binding mode of the most stable complex structure models of **1*S*** (1st entry of **1*SS'*** in Table 1) was rather similar to that of **1*R*** except for the conformation of the methyl group on the N atom.

As it can be seen from Figure 7B, the phenyl head ring (X) of **2*S*** was located in the hydrophobic pocket near Phe330, which is located deep in the gorge. The proton of the tertiary ammonium group did not interact directly with the carboxyl group of Asp72. The carbamate moiety was located near catalytic Ser200. Two CH_2-CH_2 bonds adopted a *trans* conformation. The nitrophenyl tail group (Y) was at the hydrophobic pocket opening.

Scoring or energy evaluation of ligands docked into enzyme structures is important but challenging because of the difficulty in evaluating the entropic contribution and solvation effect [27][28]. Recently, Pilger *et al*. reported the binding mode of galanthamine with AChE based on the comparison of interaction energies derived by their docking study and the predicted binding mode corresponded well to that solved by the X-ray crystal structure analysis which was in progress at the

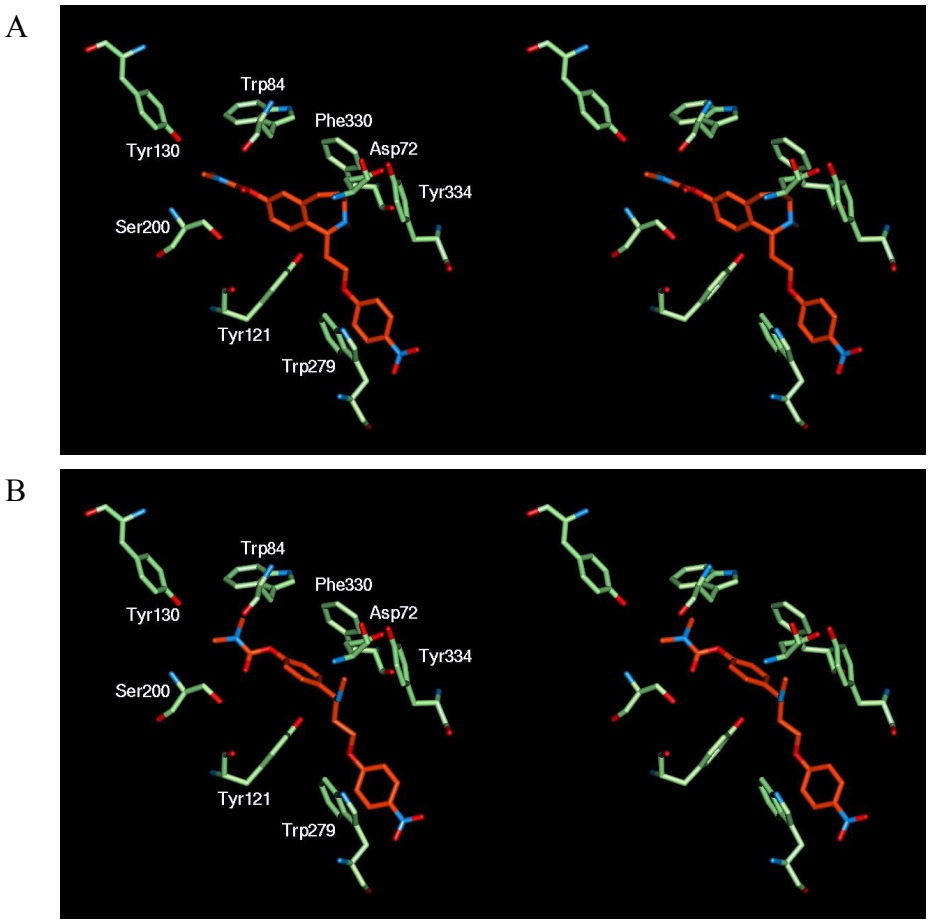

Figure 7. Complex structure models of AChE and **1*RS'*** (entry 1) (A) or **2*S*** (entry 1) (B). The front and the back are omitted for clarity.

same time [29]. In the case of one ligand or two stereoisomers of one compound such as the ones shown here or of models presented by Pilger *et al*., in which the entropic contribution and solvation effect were cancelled out, analysis of the complex structures and interaction energies derived by the docking study is considered sufficient.

3.4 Comparison among docking models of 2−4, inhibitors with different lengths of the methylene chain

The length of the methylene chain between the benzylamine and nitrophenoxy moieties (Y) is an important factor affecting the potency. Among compounds **2**−**4**, compound **3** with one methylene spacer group showed very weak inhibitory activity (IC_{50} = >1000 nM) while reasonable inhibitory activities were observed for **2** (IC_{50} = ~100 nM) and **4** (IC_{50} = 77 nM), which have two and three methylene spacer groups respectively. The binding energies among different compounds can not be directly compared with the energies presented in Table 1 since the entropy contribution and solvation effect were not considered. We therefore, focused on the position of the nitrophenyl group (Y) at the binding site. The most stable complex structure models of ***3S*** (1st entry of ***3S*** in Table 1) and ***4R*** (1st entry of ***4R*** in Table 1) obtained by the docking are shown in Figure 8.

The nitrophenyl tail group (Y) of **2** was involved in the hydrophobic interaction with the indole group of Trp279 as mentioned above. In the case of **3**, the distance between the phenyl moiety (Y)

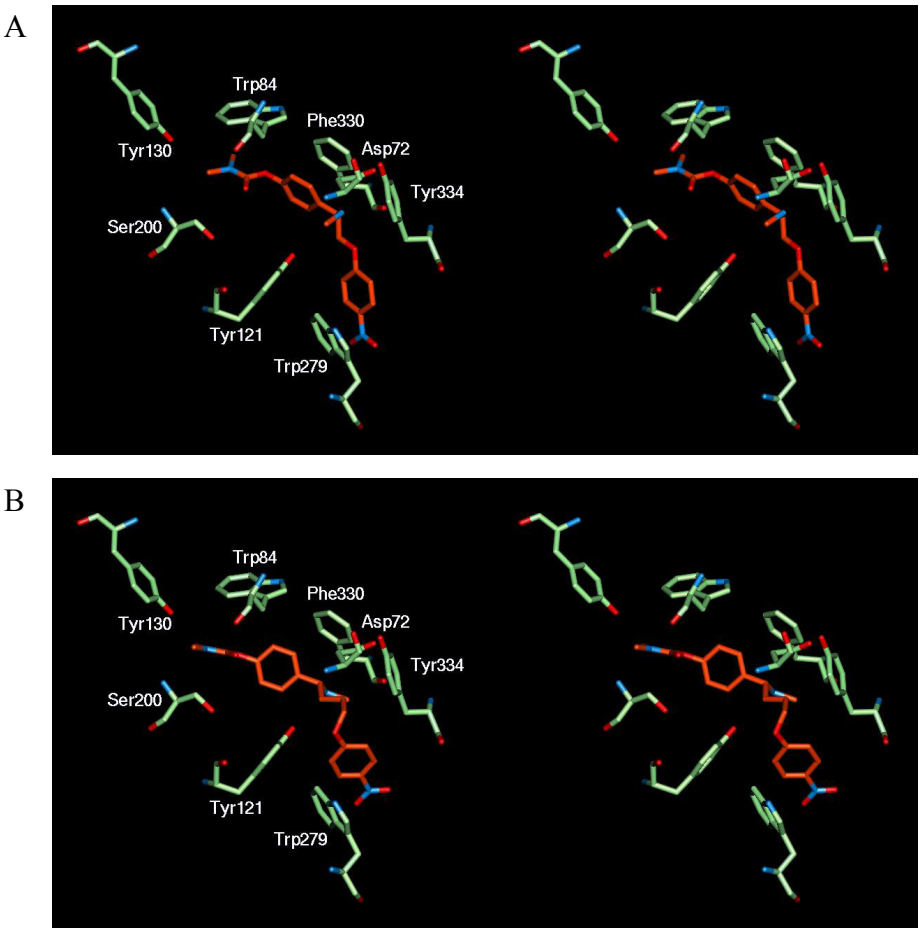

Figure 8. Complex structure models of AChE and ***3S*** (entry 1) (A) or ***4R*** (entry 1) (B). The front and the back are omitted for clarity.

and indole rings became 0.2 Å longer than that of **2** (Figure 8A). The shorter spacer length for **3**, relative to **2**, may prevent the phenyl rings X and Y to simultaneously interact with the hydrophobic pocket at the base or opening respectively, as it was the case for **2**. On the other hand, the distance between the phenyl ring (Y) of **4** and the indole ring of Trp279 was 0.4 Å shorter than that of **2** (Figure 8B), leading to an enlarged ring overlap. Moreover, the interaction at the peripheral hydrophobic site seemed to be more favorable due to the additional hydrophobic methylene group of **4** although its larger number of rotatable bonds was more disadvantageous with respect to entropy compared to **2**. This seemed to slightly lower its activity, making it the second best among the synthesized compounds.

4. Conclusion

The detailed analysis of the complex structures and on their interaction energies derived by the docking study provided a reasonable basis for the inhibition potency difference between the isomers of **1** and **2**. Furthermore, structural features of the complex models of **2**−**4** with different methylene spacer lengths corresponded well to their inhibitory activities. Although X-ray analysis of the complex is essential in determining the exact binding mode, the approach described in this article would still be very useful to understand the potencies of inhibitors based on their modeled enzyme−inhibitor interaction.

References

[1] H. J. Altman, Ed., Alzheimer's Diseases Problems, Prospects and Perspectives. Plenum Press, New York, 1987.
[2] S. B. Dunett, H. C. Fibiger, *Prog. Brain Res.*, **98**, 413-420 (1993).
[3] A. Enz, R. Amstutz, H. Boddeke, G. Gmelin, J. Malanowski, *Prog. Brain Res.*, **98**, 431-438 (1993).
[4] C. B. Millard, C. A. Broomfield, *J. Neurochem.*, **64**, 1909-1918 (1995).
[5] G. Benzi, A. Moretti, *Eur. J. Pharmacol.*, **346**, 1-13 (1998).
[6] E. Giacobini, *Jpn. J. Pharmacol.*, **74**, 225-241 (1997).
[7] C. G. Lyketsos, J. M. Sheooard, C. D. Steele, S. Kopunek, M. Steinberg, A. S. Baker, J. Brandt, P. V. Rabins, *Am. J. Psychiatry*, **157**, 1686-1689 (2000).
[8] Y.-P. Pang, A. P. Kozikowski, *J. Comput.-Aided Mol. Design*, **8**, 683-693 (1994).
[9] Y. Yamamoto, Y. Ishihara, I. D. Kuntz, *J. Med. Chem.*, **37**, 3141-3153 (1994).
[10] A. Inoue, T. Kawai, M. Wakita, Y. Iimura, H. Sugimoto, Y. Kawakami, *J. Med. Chem.*, **39**, 4460-4470 (1996).
[11] G. Kryger, I. Silman, J. L. Sussman, *Structure*, **7**, 297-307 (1999).
[12] J. L. Sussman, M. Harel, F. Frolow, C. Oefner, A. Goldman, L. Toker, I. Silman, *Science*, **253**, 872-879 (1991).
[13] H. M. Berman, J. Westbrook, Z. Feng, G. Gilliland, T. N. Bhat, H. Weissig, I. N. Shindyalov, P. E. Bourne, *Nucleic Acids Res.*, **28**, 235-242 (2000).
[14] M. Harel, I. Schalk, L. Ehret-Sabatier, F. Bouet, M. Goeldner, C. Hirth, P. H. Axelsen, I. Silman, J. L. Sussman, *Proc. Natl. Acad. Sci. USA*, **90**, 9031-9035 (1993).
[15] P. Bal-On, C. B. Millard, M. Harel, H. Dvir, A. Enz, J. L. Sussman, I. Silman, *Biochemistry*, **41**, 3555-3564 (2002).
[16] unpublished data

[17] H. Kogen, N. Toda, K. Tago, S. Marumoto, K. Takami, M. Ori, N. Yamada, K. Koyama, S. Naruto, K. Abe, R. Yamazaki, T. Hara, A. Aoyagi, Y. Abe, T. Kaneko, *Org. Lett.*, **4**, 3359-3362 (2002).
[18] QUANTA, Version 98. Accelerys, Inc., San Diego, Calif.; http://www.accelerys.com.
[19] CHARMm, Version 23. Accelerys, Inc., San Diego, Calif.; http://www.accelerys.com.
[20] B. R. Brooks, R. E. Bruccoleri, B. D. Olafson, D. J. States, S. Swaminathan, M. Karplus, *J. Comput. Chem.*, **4**, 187-217 (1983).
[21] A. Kasuya, Y. Iwata, N. Tanaka, T. Ogawa, S. Miyamoto, *Drug Des. Discovery*, **17**, 119-129 (2000).
[22] Y. Iwata, M. de Kort, R. A. J. Challiss, G. A. van der Marel, J. H. van Boom, S. Miyamoto, *Drug Des. Discovery*, **17**, 253-263, (2001).
[23] Y. Iwata, A. Kasuya, S. Miyamoto, *Drug Des. Discovery*, **17**, 231-241 (2001).
[24] M. Levitt, M.F. Perutz, *J. Mol. Biol.*, **201**, 751-754 (1998).
[25] D. A. Dougherty, D. A. Stauffer, *Science*, **250**, 1558-1560 (1990).
[26] H. M. Greenblatt, G. Kryger, T. Lewis, I. Silman, J. L. Sussman, *FEBS Letters*, **463**, 321-326 (1999).
[27] I. Muegge, Y. C. Martin, *J. Med. Chem.*, **42**, 791-804 (1999).
[28] C. Bissantz, G. Folkers, D. Rognan, *J. Med. Chem.*, **43**, 4759-4767 (2000).
[29] C. Pilger, C. Bartolucci, D. Lamba, A. Tropsha, G. Fels, *J. Mol. Graphics Modell.*, **19**, 288-296 (2001).